Electrical Power and Energy Systems 109 (2019) 122–138

Contents lists available at ScienceDirect

Electrical Power and Energy Systems

journal homepage: www.elsevier.com/locate/ijepes

A method to include component condition and substation reliability into distribution system reconfiguration

Ilias Sarantakos[a,*], David M. Greenwood[a], Jialiang Yi[b], Simon R. Blake[a], Phil C. Taylor[a,*]

[a] School of Engineering, Newcastle University, United Kingdom
[b] UK Power Networks, United Kingdom

ARTICLE INFO

Keywords:
Component condition
Condition-based failure rate
Reconfiguration
Reliability
Substation

ABSTRACT

Component condition and substation (S/S) reliability have a material impact on the cost of customer interruptions in electricity distribution systems (DSs). However, these factors are not usually considered within distribution system reconfiguration (DSR) problem formulations, because of the lack of a readily available methodology. This paper presents such a method, making use of component condition scores which are now mandatory for distribution system operators (DSOs) in the UK. Based on these condition scores, condition-based failure rate can be calculated for each component. S/S reliability is a function of component condition, S/S configuration and the network upstream of the S/Ss. The reliability of the S/S then has an impact on the reliability indices of each load point (LP) it supplies. These factors are combined to deliver a better informed algorithm for DSR, which is verified through its application on two DSs. The annual savings, compared to the formulation that neglects component condition and S/S reliability, can be in the order of tens of thousands of U.S. dollars for a single DS.

1. Introduction

Customer interruptions in power systems commonly occur within Distribution Systems (DSs) [1,2]. Deregulation has pushed the DS operators (DSOs) to reduce their expenditure by postponing investments, reducing internal expertise and decreasing maintenance frequency. Thus far, this has not had an effect on the reliability of DSs, but it may have a detrimental effect in the coming years, with the potential for the quality of supply to decline quickly [3]. It is therefore important to examine possible actions that can be taken in order to improve network reliability. DS reconfiguration (DSR) – which can be defined as the procedure of changing the topology of the network using the branch switches – is one available strategy. For each possible topology, all of the constraints should be satisfied, including the radiality of the network, as well as operational current and voltage limits. DSs are typically constructed as meshed systems but are operated in radial configuration through the use of normally open points. This is primarily to reduce the number of network components exposed to a failure on any single feeder in the case of a fault on the network [1].

Reconfiguration is usually structured as an optimization problem, with an objective to minimize power losses, voltage deviation, or load imbalance, or to maximise reliability. Optimal DSR is a combinatorial nonlinear optimization problem [4], which has often led to the use of heuristic solution algorithms, including: branch exchange method [5,6]; genetic algorithm (GA) [7–9]; particle swarm optimization (PSO) [10–12]; ant colony search algorithm [13]; cuckoo search [14,15]; invasive weed optimization [16]; and teaching-learning-based optimization [17]. Although heuristic optimization algorithms do not guarantee the optimal solution, they do identify high-quality solutions [9,18].

In [5], the objective is to reduce losses and improve load balancing through DSR. This requires a search over a number of radial configurations; therefore, two approximate power flow methods were developed to reduce the computational burden. Ch et al. [6] investigate the impact of DSR on power quality (such as voltage harmonic distortion and unbalance), along with losses, in the presence of distributed generation (DG) and reactive power sources. Tahboub et al. [8] employ a clustering algorithm to acquire representative centroids from annual load and DG profiles in order to deal with their associated variability; the corresponding objective function focusses on loss minimization. In [9], an adaptive fuzzy logic parallel GA is presented to solve the optimization problem. A paper by Guan et al. [11] considers different models of DG into the network reconfiguration problem; a decimal encoding of the decision variables is also proposed. In [15], a new methodology is developed to optimize the configuration of the network, as well as the location and size of DG. Sudha Rani et al. [16] present a multi-objective invasive weed optimization method in order to

* Corresponding author5.
E-mail addresses: ilias.sarantakos@newcastle.ac.uk (I. Sarantakos), phil.taylor@newcastle.ac.uk (P.C. Taylor).

https://doi.org/10.1016/j.ijepes.2019.01.040
Received 15 June 2018; Received in revised form 12 December 2018; Accepted 28 January 2019

Nomenclature

A, B, C	failure rate model parameters
C_{Ploss}	cost coefficient for losses (180 $/kW [23], expressed in today's U.S. dollars)
C_{jp}	interruption cost of load point (LP) p due to failure event j ($/kW)
$\text{Cost}_{\text{Ploss}}$	annual cost of active power losses ($/yr)
ECOST	total expected customer interruption cost (ECOST) of the network ($/yr)
ECOST_1	ECOST for failure events in the primary distribution system (DS) ($/yr)
ECOST_2	ECOST for failure events at substations and the upstream network ($/yr)
ECOST_{jp}	ECOST of load point (LP) p due to failure event j ($/yr)
EP	energy price ($/kWh)
$I_i^{(k)}$	nodal current injection at node i, at iteration k
I_k	current of branch k
$I_{k,\max}$	current rating of branch k
$I_{L2}^{(k)}$	current injection at node $L2$, at iteration k
$J_L^{(k)}$	branch L current at iteration k
L_p	average load of LP p (MW)
LLF	loss load factor
Loss Cost	annual cost of losses ($/yr)
N_{LP}	number of LPs
N_{b}	number of buses
$N_{\text{ev},p}$	number of possible failure events for LP p
N_{l}	number of branches
P_{C}	probability that a circuit breaker fails to open when required
P_{loss}	active power losses (calculated at peak load) (kW)
Pen	overall penalty term forcing the objective function to infinite, if there is a constraint violation
Pen_1	penalty term for loop constraints
Pen_2	penalty term for operational constraints
R_k	resistance of branch k
r	repair time (hr)
r''	maintenance outage time (hr)
r_{jp}	interruption duration of LP p due to failure event j (hr)
S_i	complex power injection at node i
Total Cost 1	total cost considering the annual cost of losses and the ECOST for the primary DS only, i.e. Loss Cost + ECOST_1 ($/yr)
Total Cost 2	total cost considering the annual cost of losses and the total ECOST, i.e. Loss Cost + ECOST ($/yr)
$V_i^{(k-1)}$	voltage at node i, at iteration k-1
$V_{\min}$, $V_{\max}$	minimum and maximum voltage limits, respectively
x	state vector
Y_i	sum of all shunt elements at node i
z	condition score (p.u.)
Z_L	series impedance of branch L
λ	failure rate (f/yr) [for lines/cables (f/yr·km)]
λ''	maintenance outage rate (out/yr)
λ_{A}	active failure rate (f/yr) [for lines/cables (f/yr·km)]
λ_{P}	permanent (total) failure rate (f/yr) [for lines/cables (f/yr·km)]
λ_j	failure rate of failure event j

simultaneously minimize losses, maximum node voltage deviation, number of switching operations, and the load balancing index; they also implement a backward/forward sweep load flow for the power flow calculations. An advantage of the optimization methods in [14,15,17] – cuckoo search and teaching-learning-based optimization – is that they have few control parameters.

As mentioned earlier, DSR involves a search over a number of network configurations; the size of the search space of the problem is related to the encoding of the state vector, i.e. what each decision variable represents [19]. The state vector in DSR represents a specific network topology. Two options are presented in [20]. The first option (binary encoding) assumes that each decision variable represents the status (open/closed) of the corresponding branch. The length of the state vector, in this case, is equal to the number of branches that are involved in the network reconfiguration. The second option (integer encoding) considers that the network consists of a number of loops and each decision variable represents the integer index of the branch that breaks each loop; in this case, the length of the state vector is defined by the number of loops. These two options are compared in [20], and it is shown that the second alternative outperforms the first one in optimization time and number of objective function evaluations. The former approach is followed in [8] and [10], which use a binary GA and PSO, respectively; whereas the latter approach is followed in [11,15–17], and it is stated that it can reduce the number of state variables, generate fewer infeasible solutions, and have better search efficiency.

From the perspective of reliability, Brown et al. [21] extended the use of DSR to improve DS reliability. In [10], probabilistic reliability models are applied to assess the reliability at the load points (LPs) and the DSR problem is formulated in a multi-objective framework, considering power loss and reliability. Paterakis et al. [22] also propose a multi-objective optimization method, which minimizes active power losses and one of three commonly used system reliability indices. It is not uncommon to disregard customer interruption costs entirely [10,22]. In [7,23–25], an aggregate objective function is considered, which takes account of losses and reliability concurrently by expressing the objective in monetary terms via electricity price and customer interruption costs.

However, the aforementioned publications neglect component condition (see Section 2) when evaluating network reliability and use average failure rates that depend only on the type of the components regardless of their condition. Furthermore, the available literature on DSR deals with networks that have only one substation (S/S) or, in cases where multiple S/Ss are present, the problem is formulated such that a single S/S is considered. Consequently, either the reliability of the S/Ss is not considered in network reconfiguration studies or they are assumed to be perfectly reliable. Moreover, average customer interruption costs [7,24] or composite customer damage functions [25] are considered, in order to convert customer interruptions to cost, for all LPs. In fact, the expected customer interruption cost (ECOST) depends on customer type and outage duration; two LPs can yield significantly different ECOSTs even if they have the same power demand and are interrupted for the same amount of time [1,26].

The main contributions of this paper are to take component condition and substation reliability into account within the DSR problem. Condition-based failure rates are used to determine the reliability of the network compared to the standard approach using average failure rates. Networks with multiple S/Ss are considered and their reliability is determined by component condition, S/S configuration, and the network upstream of the S/Ss, which can lead to different reliability indices for the S/Ss supplying a given DS. The proposed objective function is an aggregate function, which considers reliability and power losses and is expressed in monetary terms. Reliability is taken into account through the ECOST, which is calculated not only for interruptions that come from the primary DS (network between the distribution S/Ss and the distribution transformers (TXs)), but also for outages that are caused by the S/Ss and the upstream network. Finally, each LP has a specific customer type and the associated customer damage function (CDF).

The model used in this paper considers constant loads; specifically

average load values for reliability evaluation, and peak values – along with a loss load factor – for cost of losses. The reliability of the system and the cost of losses are calculated for a yearly period – but this does not preclude the application of the proposed method to more discrete time periods. For example, in the case of a planned maintenance of an S/S transformer or if new condition data become available to the DSO, then the methodology presented in this paper can be implemented in order to find a better informed optimal network configuration for the given time interval. This work does not focus on the optimization method, because the main aim of this study is to demonstrate the value of including component condition and S/S reliability into the DSR problem.

This paper is based on the following assumptions:

(1) Constant load model (peak and average values are used).
(2) Balanced three-phase system.
(3) Substation transformer tap changer positions are fixed.
(4) Uncertainty is not considered.
(5) Common mode failures are not taken into account.

The rest of the paper is organized as follows: Section 2 gives an overview of component condition assessment and Section 3 explains reliability evaluation of the network. Section 4 presents the problem formulation and describes the solution procedure. Then, in Section 5, the proposed methodology is applied to two DSs and the simulation results are presented and discussed. Finally, the conclusions are drawn in Section 6.

2. Component condition

Network reliability models generally use average component failure rates. However, there are a number of methodologies and asset management decision support tools that relate specific component condition parameters to a single value, known as a health index (HI), indicating its overall condition [27]. The condition parameters can be assessed and assigned a score using maintenance or condition monitoring data, which will become more prevalent in smart networks and modern S/Ss. HIs and their associated condition-based failure rates can be derived and, together with CDFs for each LP, the ECOST can be calculated.

The process that is generally followed by many component condition assessment methodologies in order to derive the component HI (overall condition score) is illustrated in Fig. 1. Based on the HI, some methodologies classify the component into one of several predefined HI categories, accompanied by a qualitative description for its condition, probability of failure, and expected remaining life [28–30]; a number of alternative methodologies also convert the component HI into a failure rate [31–35].

In the UK, the gas and electricity regulator (Ofgem) approved in 2017 a common methodology (CNAIM) [35] across all DSOs for the evaluation, forecasting, and regulatory reporting of component condition (health scores) and associated risks. This will encourage DSOs to collect and utilize condition data in a more systematic way. Consequently, DSOs will have better knowledge and understanding of the condition of their assets, which could facilitate the application of the proposed methodology to a DS.

In order to incorporate a condition assessment methodology into this paper, it needs to satisfy the following requirements: (1) it should be reproducible; many methodologies are described qualitatively (some of them constitute intellectual property), and thus cannot be implemented, (2) it must cover all basic types of components; some methods deal only with a specific component type (mainly transformers), and (3) it should relate the component HI (or condition score) to the corresponding condition-based failure rate. From all of the above-mentioned methodologies, only Brown et al. [33] and CNAIM [35] satisfy the criteria stated; however CNAIM accounts for only condition-based failures and would require the contribution of non-condition-based failures in order to yield overall failure rates. Consequently, the methodology in [33] has been chosen for component condition assessment in this paper, and is described below.

Brown et al. [33] describe a method to convert component condition data into failure probabilities. The method begins with assessment of selected condition parameters by assigning a score to each, using component inspection data: the condition parameters for most network components can be found in [35]. Subsequently, according to the weight of each criterion, an overall condition score is derived for the component. Then, using an empirically derived equation (1), the condition-based failure rate can be computed.

$$\lambda(z) = Ae^{Bz} + C \tag{1}$$

Condition scores range from 0 to 1, which correspond to the best and the worst condition, respectively. The failure rate functions (with respect to condition) for power transformers (less than 25 MVA), circuit breakers (CBs), underground cables, overhead lines, and busbars are illustrated in Fig. 2.

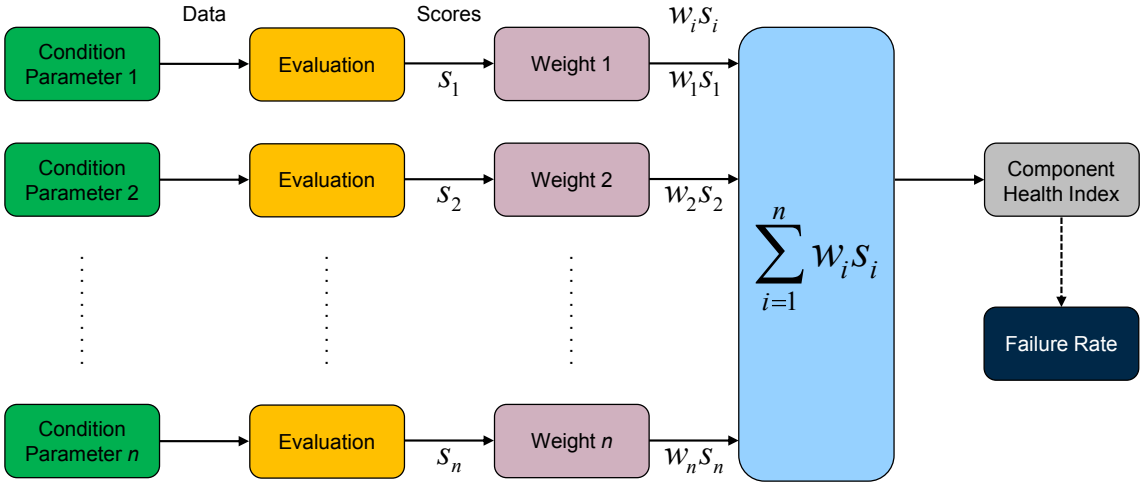

Fig. 1. Concept of HI calculation. A number of condition parameters are assessed and according to their corresponding weights, an overall condition score is computed. Some methodologies also derive a failure rate based on the component HI.

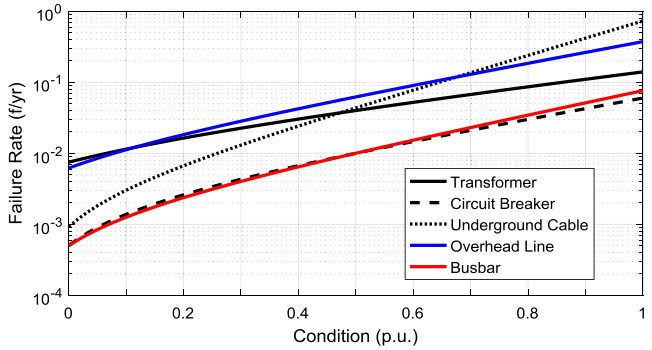

Fig. 2. Specific component failure rate functions (failure rate for lines/cables in f/yr·km). These are derived using (1) and coefficients, which can be found in [33].

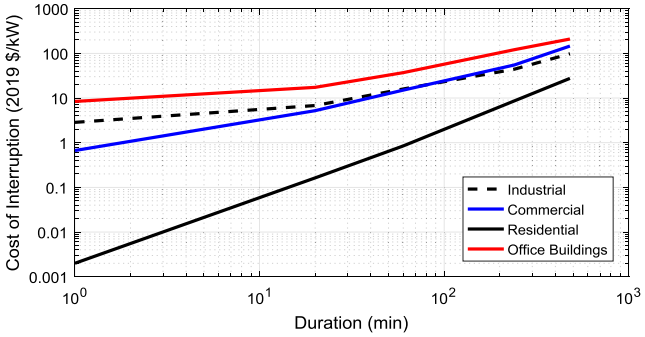

Fig. 3. CDFs used to represent the cost of interruption for different customer types.

3. Reliability evaluation

This paper uses a reliability model that takes account of both the primary DS and S/Ss, which are analyzed in Sections 3.1 and 3.2, respectively. The minimal cut set method is used to assess the network reliability [1,36]. A minimal cut set is a set of components which, when all of them are out of service, an outage is caused to a specific LP. However, there is not an interruption of service, when at least one of these components remains operational. There are two failure modes for a component: passive and active. Passive events do not cause operation of the CBs and consequently do not affect any other healthy components, whereas active events cause the protection breakers to operate and a number of other healthy components are removed from service [1]. The following failure modes were considered in this study:

(1) First-order permanent (total) failures (passive and active failures).
(2) First-order active failures.
(3) First-order active failures with stuck CBs.
(4) Second-order overlapping permanent failures (including maintenance).

The corresponding equations for the reliability indices of the above failure modes can be found in [1].

When all possible failure events and the LPs that are affected by each of them have been identified, the ECOST can be calculated. For each LP p and for each outage event j, the ECOST_{jp} is calculated as follows [1,26]:

$$\text{ECOST}_{jp} = C_{jp}(r_{jp})L_p\lambda_j \tag{2}$$

The summation of ECOST_{jp} for all LPs and all failure events yields the total ECOST of the network.

$$\text{ECOST} = \sum_{p=1}^{N_{LP}} \sum_{j=1}^{N_{ev,p}} C_{jp}(r_{jp})L_p\lambda_j \tag{3}$$

The interruption cost C_{jp} is a function of the interruption duration and is calculated using the CDF of each LP. Fig. 3 presents interruption cost estimates for various customer types and outage durations. These values are taken from [37] and are expressed in today's (2019) U.S. dollars.

3.1. Primary DS

A primary DS is the section of a network between the distribution S/Ss and the distribution transformers and comprises primary feeders which emanate from the low voltage buses of the distribution S/Ss [2]. These networks are operated in radial configuration; all of the minimal cut sets consist of a single component (line or CB) for each LP of the system. To demonstrate the reliability evaluation model for the primary DS, this was applied to one feeder (F2) of the RBTS Bus 4 DS [38], which is presented in Fig. 4. In this network, there are disconnect switches at both ends of the main feeder sections and fuses in each lateral distributor. These components are not shown in Fig. 4 and are considered perfectly reliable. Disconnect switches are generally not capable of breaking short-circuit currents and are used for isolation.

An active failure along the main feeder causes the CB to operate to clear the fault, interrupting all LPs supplied by the feeder until the CB is reclosed. The time required to detect and isolate the fault is called switching time. After the CB has been reclosed, the power supply between the supply point (SP) and the point of isolation is restored. The LPs downstream of the faulted branch are restored following a repair, unless they can be transferred onto another feeder through a normally open point.

If a fault occurs on a lateral distributor its fuse blows, causing the outage of the corresponding LP until the failed component is repaired. However, in this case, no other LPs are interrupted.

The failure of a feeder CB results in an outage of all LPs of the feeder. The failed CB must be repaired in order to restore the interrupted LPs unless an alternative supply is available.

To clarify the cases and processes above, Table 1 presents a reliability analysis for LP 9. Component reliability data were taken from [38] and LP 9 was considered to be an industrial customer with an average demand of 1.5 MW. The ECOST was calculated using (2) and the CDF for industrial customers.

In Table 1, r is the LP outage time, which is equal to the component repair time if the LP cannot be transferred, or equal to the switching time (assumed to be 1 hr) if the LP can be transferred.

3.2. Substations

S/Ss are the sources of the primary DS and are significant elements of power systems; their failure can lead to an outage at all LPs supplied by the failed S/S. To evaluate the reliability of S/Ss, three factors are considered in this paper: component condition, S/S configuration, and the network upstream of the S/Ss. The first factor was discussed in Section 2; Sections 3.2.1 and 3.2.2 demonstrate the contribution of the other two factors to S/S reliability.

3.2.1. Substation configuration

The arrangement of an S/S has an impact on its reliability indices. Two typical configurations [1] are shown in Fig. 5. In configuration (a), the low voltage bus, 7, is fed by two subtransmission lines, 1 and 4, through transformers, 2 and 5. The low voltage side of each transformer is connected to a CB (3 and 6). In configuration (b) the low voltage busbars, 7 and 8, are split by a normally open bus section CB.

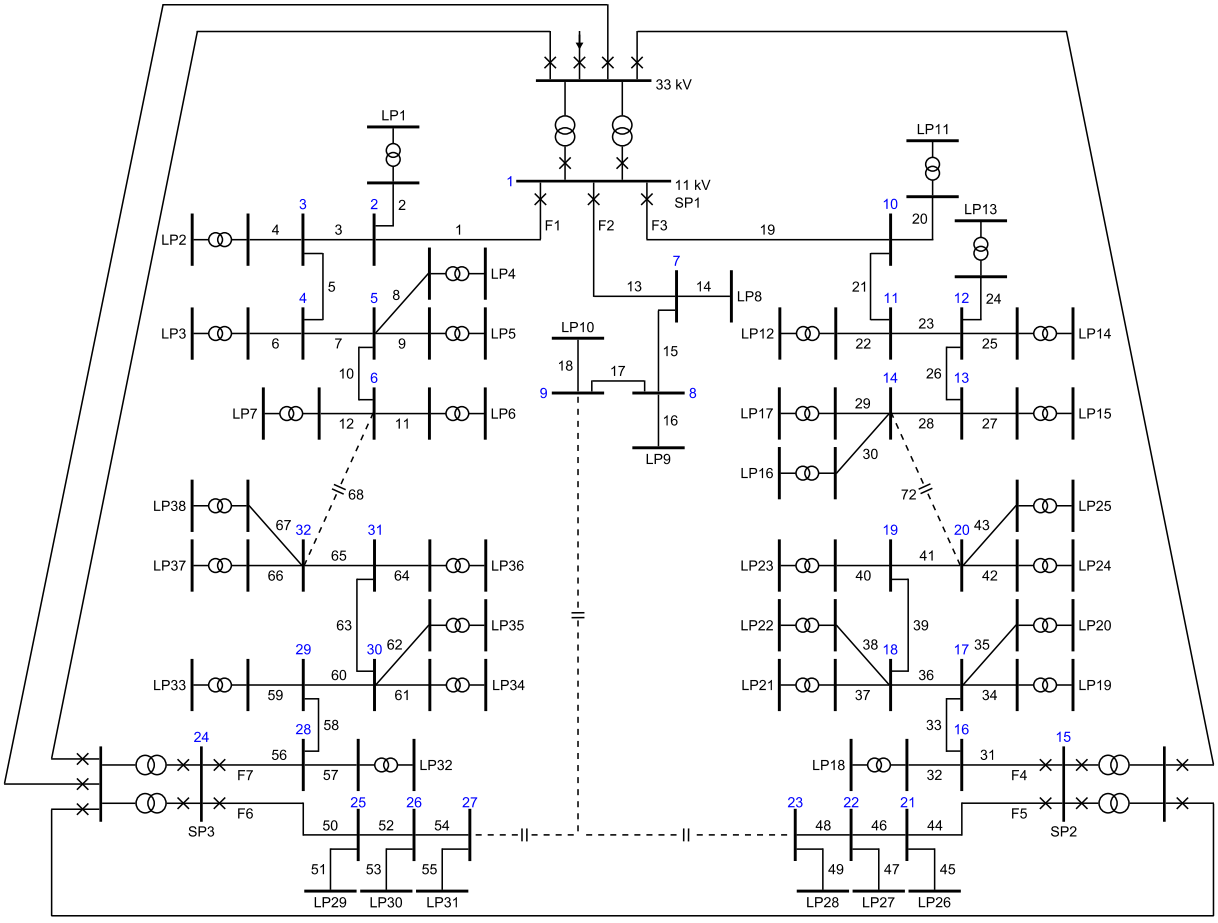

Fig. 4. The RBTS Bus 4 DS (Branch numbers are shown in black; bus numbers are shown in blue).

Table 1
Results for load point 9 of the RBTS Bus 4 DS.

Component type	Component failure	λ (f/yr)	No alternative supply		Alternative supply	
			r (hr)	ECOST (k$/yr)	*r* (hr)	ECOST (k$/yr)
Main feeder	13	0.0520	5.00	4.453	1.00	1.244
	15	0.0520	5.00	4.453	1.00	1.244
	17	0.0390	1.00	0.933	1.00	0.933
Distributor	16	0.0488	5.00	4.179	5.00	4.179
CB	F2 CB	0.0060	4.00	0.398	1.00	0.144
Total	–	0.1978	4.18	14.416	1.99	7.744

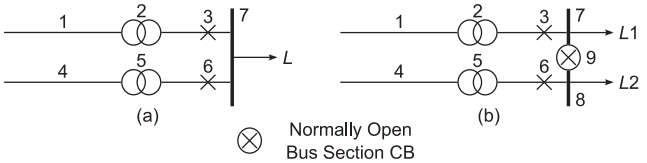

Fig. 5. Typical substation configurations: (a) shows a single low voltage bus, while (b) shows two low voltage buses separated by a normally open bus section CB.

These configurations were analysed using component reliability data from [38], which are shown in Table 2. Every failure mode was included in the analysis for each configuration. The results of the reliability analysis are shown in Table 3 (see Appendix A for detailed calculation). The results correspond to four cases:

Table 2
Component reliability data.

Component	λ_P	λ_A	λ''	*r*	*r*″	P_C
33/11 kV TX	0.0150	0.0150	1.0	15	120	–
11/0.4 kV TX	0.0150	0.0150	–	10[a]	–	–
33 kV CB	0.0020	0.0015	0.5	4	96	0.05
11 kV CB	0.0060	0.0040	1.0	4	72	0.05
33 kV busbar	0.0010	0.0010	0.5	2	8	–
11 kV busbar	0.0010	0.0010	1.0	2	8	–
33 kV line	0.0460	0.0460	0.5	8	8	–
11 kV line	0.0650	0.0650	–	5	–	–

[a] Replacement time by a spare (hr).

Table 3
Substation reliability analysis results.

Substation configuration	Case	λ (f/yr)	*r* (hr)	ECOST (k$/yr)
Config. (a) – Load L (F4 and F5)	(1)	0.0722	2.04	9.188
	(2)		1.47	6.957
	(3)		1.00	4.549
	(4)		0.43	2.318
Config. (b) – Load L1 (Feeder F4)	(1)	0.2724	1.26	6.326
	(2)		0.47	3.009
	(3)		1.00	4.127
	(4)		0.17	0.794
Config. (b) – Load L2 (Feeder F5)	(1)	0.2670	1.27	15.927
	(2)		0.47	7.633
	(3)		1.00	12.776
	(4)		0.17	4.482

(1) Non-automated S/S and no alternative supply;
(2) Automated S/S (with an S/S switching time of 10 min) and no alternative supply;
(3) Non-automated S/S and alternative supply;
(4) Automated S/S and alternative supply.

S/S automation was taken into account through S/S switching time, which is the time required to perform the switching actions at an S/S following a failure. S/S switching time affects the outage duration for active and active + stuck CB failures, which are the highest contributors to the S/S failure rate (see Appendix A); therefore, S/S automation has a significant impact on the ECOST, namely $ECOST_2$. First-order permanent and second-order overlapping permanent failures (including maintenance) require the repair of those failed component(s) in order to restore at least one incoming circuit; thus, their consequences are not mitigated by S/S automation.

For each failure event, the failure rate, the outage time and the ECOST were calculated. For the calculations, the S/S (each configuration) was assumed to be connected to SP2 of the RBTS Bus 4 DS, which supplies feeders F4 and F5, loaded at 4.01 MW and 3 MW respectively. The sub-transmission line length was assumed to be 5 km.

Table 3 shows that different S/S configurations lead to different reliability indices and outage costs. S/S automation and alternative supply play an important role in determining the average outage duration of an S/S and the corresponding ECOST. The analysis also indicates: (1) the importance of considering active failures and stuck-breaker conditions, which depend on component condition; (2) the impact of subtransmission lines on S/S reliability; and (3) the effect of component maintenance.

If a CB fails to open, other CBs further from the failed component are activated; this might cause a greater part of the network, and more LPs, to be interrupted. Some of the failure events considered involve components that belong to the primary DS but cause the outage of the entire low voltage bus of the S/S; this is why it is critical to include these events in the analyses. These events are active failures of the feeder CBs (e.g. F4 CB) and active failures on main feeder sections in combination with a stuck CB (e.g. (44, 46, 48)A + F5 CB S), which exhibit the interaction between S/Ss and the primary DS.

Table 4
Impact of upstream network on substation reliability.

Failure event	Number	λ (f/yr)	*r* (hr)	ECOST (k$/yr)
Supply point SP1				
First-order	2	2.00×10^{-3}	2.00	0.3099
Second-order	4	1.19×10^{-6}	5.93	0.0007
Second-order (m)	4	9.21×10^{-4}	10.37	0.9781
Active failure	10	5.45×10^{-2}	1.00	4.6458
Active + stuck	6	9.22×10^{-2}	1.00	7.8617
Total		1.50×10^{-1}	1.07	13.7961
Supply point SP2				
First-order	3	3.00×10^{-3}	2.00	0.3362
Second-order	16	3.93×10^{-4}	3.99	0.0806
Second-order (m)	16	1.17×10^{-2}	7.40	5.3777
Active failure	15	9.15×10^{-2}	1.00	5.7647
Active + stuck	8	1.38×10^{-1}	1.00	8.7084
Total		2.45×10^{-1}	1.32	20.2676
Supply point SP3				
First-order	3	3.00×10^{-3}	2.00	0.3403
Second-order	4	1.19×10^{-6}	5.93	0.0004
Second-order (m)	4	9.21×10^{-4}	10.37	0.6428
Active failure	16	9.30×10^{-2}	1.00	6.0214
Active + stuck	8	1.84×10^{-1}	1.00	11.9229
Total		2.81×10^{-1}	1.04	18.9278

(m) represents total outages overlapping a maintenance outage.

3.2.2. Upstream network

Even if two S/Ss have the same configuration and the condition of their components is identical, a difference in their upstream network can result in different reliability indices. To demonstrate this, the network upstream of the S/Ss of the RBTS Bus 4 DS (see Fig. 6) was used as an example. Table 4 shows the results of the analysis.

Fig. 6 shows S/Ss 2 and 3 are fed through the 33 kV busbar of S/S 1. Therefore, it is expected that the failures rates of S/Ss 2 and 3 will be higher than the failure rate of S/S 1, as confirmed by Table 4. S/S 3 is supplied by three 33 kV lines, two of which are 15 km long. It can be deduced that their active failures, in combination with a stuck CB, are major contributors to the corresponding failure rate. This is why S/S 3 has the highest failure rate, illustrating the importance of the upstream

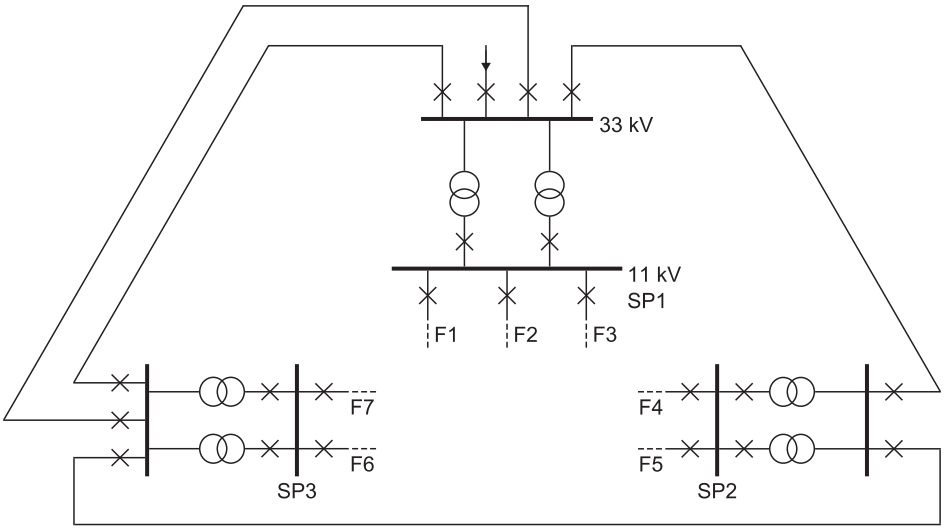

Fig. 6. Upstream network of the RBTS Bus 4 DS.

network. S/S 2 is supplied by two 33 kV lines, which are 10 km long each, resulting in smaller contributions to the S/S failure rate by active + stuck failures compared to S/S 3. However, second-order outages (including maintenance) have a significantly higher contribution to the S/S failure rate, and an even larger impact on the ECOST.

Finally, the network downstream of the S/Ss has an impact on S/S reliability as well. This happens through main feeder section active failures in combination with a stuck feeder CB. This impact is small compared to the three aforementioned factors and this is why it is not analyzed separately, however it is considered in this study.

4. Problem formulation and solution method

4.1. Problem formulation

The goal of DSR is to find a radial configuration which optimizes a specific objective function whilst satisfying operational constraints. This proposed objective function and the relevant constraints are described in this section.

4.1.1. Objective function

This paper proposes an aggregate cost function, comprising the annual cost of active power losses and the ECOST. The ECOST takes into account outages in the primary DS, and failures at S/Ss and the upstream network, while also considering the condition of network components through the use of condition-based failure rates within the reliability evaluation. The proposed cost objective function provides a balance between active power losses and network reliability, both of which are important issues to DSOs [25]. The objective function is as follows:

$$\min f = \mathrm{Cost}_{\mathrm{Ploss}} + \ \mathrm{ECOST} + \mathrm{Pen} \tag{4}$$

The first term of (4) can be evaluated as follows [27]:

$$\mathrm{Cost}_{\mathrm{Ploss}} = C_{\mathrm{Ploss}} \cdot P_{\mathrm{loss}} = (8760 \cdot \mathrm{LLF} \cdot \mathrm{EP}) \cdot \sum_{k=1}^{N_l} |I_k|^2 R_k \tag{5}$$

4.1.2. Topology constraints

The state vector (x) in DSR corresponds to a certain network configuration. The way decision variables are coded clearly affect the efficiency of the optimization algorithm [19]. In [20], a binary and a decimal encoding are presented. A binary encoding means that each decision variable represents the branch status – 0 for open, and 1 for closed; it is obvious that the number of (reconfigurable) branches defines the length of the state vector in this case. A decimal encoding requires the identification of the fundamental loops of the network, and then each decision variable represents the open branch of each loop (in order to ensure a radial configuration); the length of the state vector in this case is equal to the number of loops. In the RBTS Bus 4 DS (see Fig. 4), the size of the search space for binary encoding is $2^{34} = 1.718\mathrm{e} + 10$, while the corresponding size for integer encoding is $11 \times 7 \times 7 \times 7 \times 11 = 41{,}503$. Therefore, decimal encoding can substantially reduce the infeasible solution ratio, and thus improve the efficiency of the optimization algorithm (regardless of the method per se) [11].

In this study, integer encoding is adopted and it is applied to the RBTS Bus 4 DS in order to make it more comprehensible. In this network, only the main feeder sections are involved in the reconfiguration, since the disconnection of a lateral distributor would cause the isolation of an LP regardless of the wider network configuration. The loops of the network are shown below:

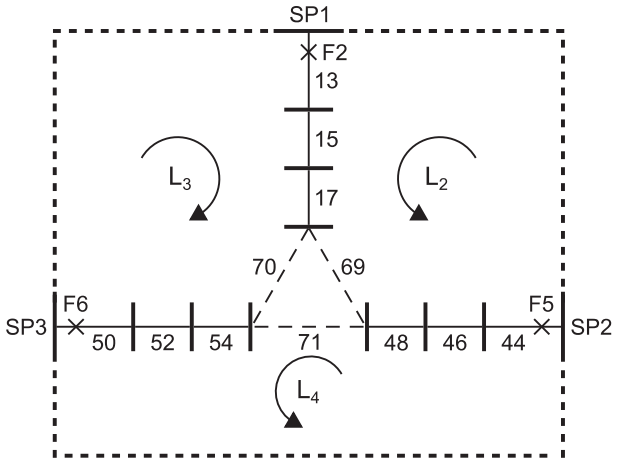

Fig. 7. Part of the RBTS Bus 4 DS (Loops 2–4, comprising F2, F5, and F6).

L_1 : {1, 3, 5, 7, 10, 68, 65, 63, 60, 58, 56}
L_2 : {13, 15, 17, 69, 48, 46, 44}
L_3 : {13, 15, 17, 70, 54, 52, 50}
L_4 : {44, 46, 48, 71, 54, 52, 50}
L_5 : {19, 21, 23, 26, 28, 72, 41, 39, 36, 33, 31}

where branches 68–72 represent the normally open points between F1-F7, F2-F5, F2-F6, F5-F6, and F3-F4, respectively. It has been assumed that F2, F5, and F6 are interconnected through single branches as shown in Fig. 7.

The branches of each loop are renumbered sequentially and therefore the decision variables are constrained as follows:

$$\begin{aligned} &1 \leqslant x_1, x_5 \leqslant 11 \\ &1 \leqslant x_2, x_3, x_4 \leqslant 7 \end{aligned} \tag{6}$$

where x_i, $i = 1, 2, \ldots, 5$ represents the branch that is selected to break the loop i; generally, the state vector is $x = (x_1, x_2, \ldots, x_n)$, where n is the number of loops in the network under study, for example, if $x = (5, 3, 4, 4, 5)$, the open branches of the network are the following: 10, 17, 70, 71, and 28.

The above constraints (6) are not sufficient to guarantee a feasible network configuration. Some non-smooth constraints are required to ensure connectivity of the network and that no loops are created. There can be multiple common branches between loops [12,20] and this has to be taken into account. In this network, there are three loops (see Fig. 7), that each two of them have branches in common. More specifically, branches {13, 15, 17}, {44, 46, 48}, and {50, 52, 54} are common between loops L_2 - L_3, L_2 - L_4, and L_3 - L_4, respectively. The first non-smooth constraint accounts for common branches between two loops. This means that from the above-mentioned sets of branches, not more than one branch from each set can be selected, e.g. if, branch 13 is open, then branches 15 and 17 should be closed. This topology (three loops, that each two of them have common branches) necessitates an additional non-smooth constraint, which is not mentioned in [12,20]: not more than two branches of these sets can be selected, e.g. if branches 17 and 48 are open, then branches 50, 52, and 54 should be closed. Otherwise, a number of LPs would be isolated. These constraints can be written as:

$$\mathrm{Pen}_1 = \begin{cases} \infty, \text{ loop constraints violation} \\ 0, \text{ otherwise} \end{cases} \tag{7}$$

4.1.3. Operational constraints

The network must respect operational voltage (8) and current (9) limits, which are enforced via a penalty constraint (10):

$$V_{\min} \leqslant |V_i| \leqslant V_{\max}, \ \ i = 1, 2, \ \ \ldots, N_b \tag{8}$$

Table 5
GA parameters.

Parameter	Value
Population size	50 (Case Study 1)/100 (Case Study 2)
Maximum generations	100
Maximum stall generations	30
Number of runs	2

$$|I_k| \leqslant I_{k,\max}, \quad k = 1, 2, \quad \ldots, N_l \tag{9}$$

$$\mathrm{Pen}_2 = \begin{cases} \infty, \text{ operational constraints violation} \\ 0, \text{ otherwise} \end{cases} \tag{10}$$

The aforementioned penalty terms can thus be combined:

$$\mathrm{Pen} = \mathrm{Pen}_1 + \mathrm{Pen}_2 \tag{11}$$

4.2. Solution method

Optimal DSR is a nonconvex mixed-integer nonlinear programming problem. Integer variables are introduced by the branch switches, through which the reconfiguration is implemented. Nonlinearity is introduced by the power-flow equations and the ECOST. These factors lead to a heavy computational burden, especially when the network under consideration is large [8]; this has often led to the use of metaheuristics to solve the problem.

As far as the proposed solution approach is concerned, much weight is placed on the reduction of the size of the search space of the problem. A binary encoding of the decision variables (open/closed status) leads to a high infeasible solution ratio; a decimal encoding can generate far fewer infeasible solutions, and therefore reduces the optimization time. Moreover, the formulation of extra (non-smooth) constraints, due to the existence of common branches between loops, reduces the number of power flow calculations – these of infeasible configurations – and in turn further decreases the computational time.

The problem formulation presented in this paper can be used with any heuristic optimization algorithm. The GA has been selected in this work because it is an effective algorithm for large-scale combinatorial optimization problem and has been extensively used in the relevant literature [7–9]. It should also be noted that the *Integer ga* solver [39] used in this paper is based on a modified and improved GA for solving integer and mixed integer optimization problems [19]. The performance of the optimization algorithm is presented in Section 5.4 and is also compared to PSO.

The state vector, objective function, and constraints of the problem were explained in Section 4.1. The problem has been formulated in MATLAB and the selected parameters for the GA are shown in Table 5. The stopping criterion for the algorithm is when the number of

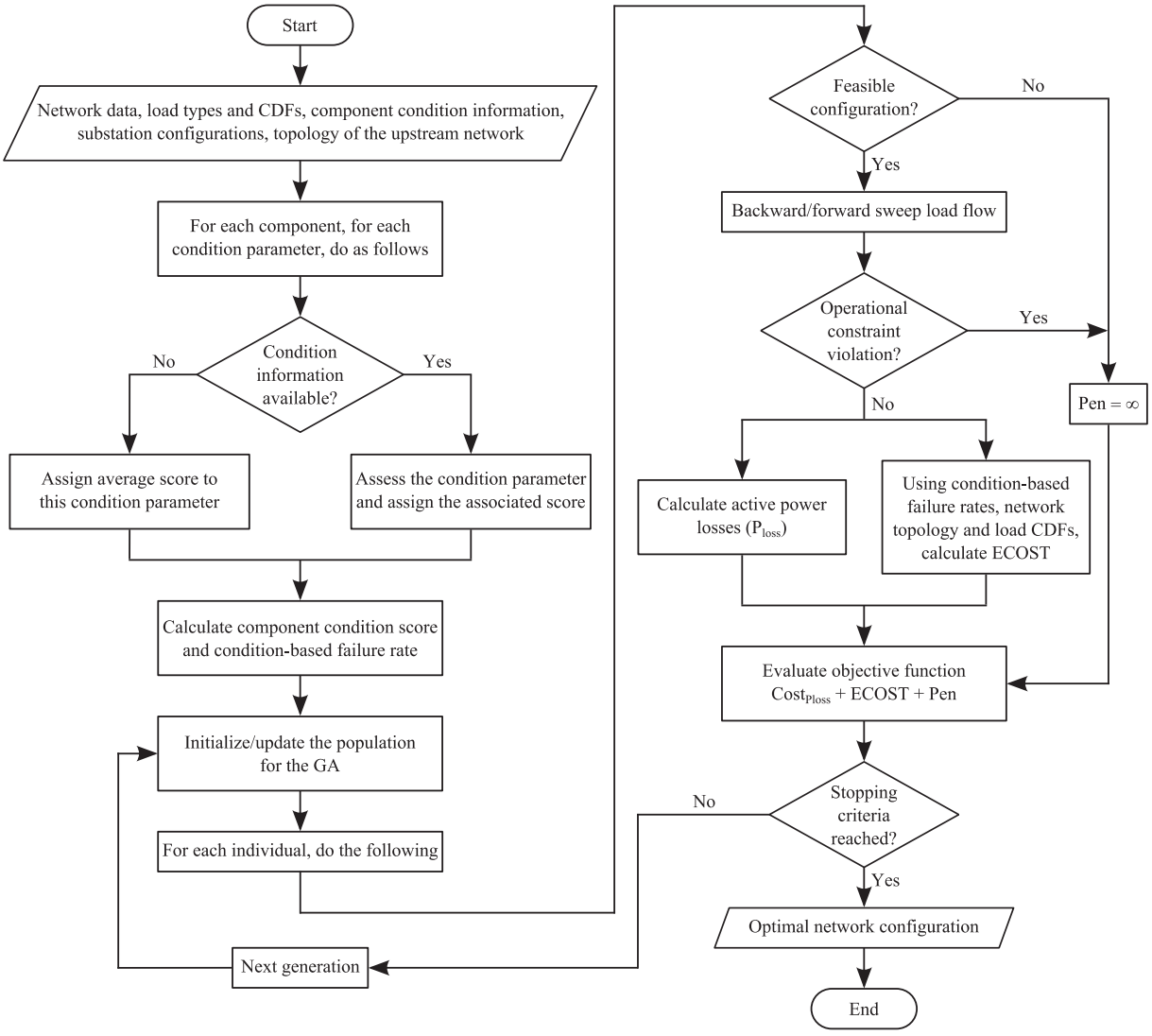

Fig. 8. Flowchart of the proposed approach.

generations reaches *maximum generations*; however the GA will also stop if there is no change in the best objective function value in a sequence of generations equal to *maximum stall generations*. The flowchart of the overall procedure is presented in Fig. 8.

The power flow calculation for radial DSs are solved via a backward/forward sweep method, using MATPOWER [40]. Backward/forward sweep methods have been widely used in the relevant literature, e.g. [6,16,22], and are thoroughly explained in [41,42]. The method used in this paper is briefly described below:

(1) Number the branches of the network such that branches located further from the root (substation) correspond to greater indices. This means that layers are considered as moving away from the root; and in order to number the branches of the next layer, all branches in the previous one must have already been numbered.
(2) Set all bus voltage magnitudes to the given voltage at the root node (flat start).
(3) Calculate nodal currents at iteration k, as follows:

$$I_i^{(k)} = \left(\frac{S_i}{V_i^{(k-1)}}\right)^* - Y_i V_i^{(k-1)},\ i = 1, 2, ...,N_b \tag{12}$$

(4) Backward sweep: Starting from the branches in the last layer and moving towards the root, update the upstream branch current as in (13). $L1$ and $L2$ are assumed to be the sending and receiving ends of branch L, respectively.

$$J_L^{(k)} = -I_{L2}^{(k)} + \sum \begin{pmatrix} \text{branch currents} \\ \text{originating} \\ \text{from node } L2 \end{pmatrix},\ L = N_l, N_l - 1, ...,1 \tag{13}$$

(5) Forward sweep: Starting from the branches in the first layer and heading towards the ones in the last, update the receiving end voltage, for each branch L, as follows:

$$V_{L2}^{(k)} = V_{L1}^{(k)} - Z_L J_L^{(k)},\ L = 1, 2, ...,N_l \tag{14}$$

(6) Repeat steps 3, 4, and 5, until convergence is achieved.

5. Case studies

The proposed DSR methodology was applied to two networks to demonstrate the value of incorporating component condition and S/S reliability into the DSR formulation. The following assumptions were made for both case studies:

(1) Condition-based failure rates are derived as illustrated in Fig. 2;
(2) CBs and overhead lines in Fig. 2 are assumed to represent 11 kV components;
(3) Failure rates for 33 kV (the upstream network voltage) components (CBs and lines) have been considered to be smaller than their 11 kV counterparts by the same proportion as in Table 2; the average failure rate for an 11 kV CB is assumed to be 0.01 f/yr, whereas the corresponding value for a 33 kV CB is 0.0033 f/yr. For overhead lines, the average failure rate is considered to be 0.062 f/yr·km at 11 kV, and 0.044 f/yr·km at 33 kV;
(4) CB failure rates illustrated in Fig. 2 are total failure rates and the associated active failure rates can be calculated using the ratio between these parameters in Table 2. Consequently, the average active failure rates for an 11 kV and a 33 kV CB are assumed to be 0.0067 f/yr and 0.0025 f/yr, respectively;
(5) Component reliability data apart from failure rates are taken from Table 2;
(6) All main feeder sections and laterals are considered as overhead lines, unless otherwise stated;
(7) Overhead line conductors are assumed to be ACSR 477 kcmil ($R = 0.143\ \Omega$/km).

Table 6
Substation failure rates (Test Case 1).

Substation	S/S 1	S/S 2	S/S 3
Failure rate (f/yr)	0.2313	0.3878	0.4012

5.1. RBTS Bus 4 DS

These case studies used the RBTS Bus 4 DS [38], an 11 kV DS supplied by three 33/11 kV S/Ss, as shown in Fig. 4. It has seven feeders, 29 normally closed branches (sectionalizing switches) and 5 normally open branches (tie switches).

The following modifications and assumptions have been made for the RBTS Bus 4 DS:

(1) LPs 8–10 and 26–31 were industrial and LPs 24 and 25 were office buildings;
(2) Alternative supply was available for all LPs (after switching), following a fault on a feeder or an S/S failure;
(3) The failure rate for all distribution transformers was considered to be 0.015 f/yr;
(4) Distribution transformers could be replaced by a spare following a failure;
(5) The length of branches 68–72 was assumed to be 0.75 km;
(6) Power factor for all LPs was 0.98 lagging.

The impact of the upstream network and the condition of S/S components on DSR is demonstrated through the following two test cases.

5.1.1. Test Case 1

This test case investigated the impact of the network upstream of the S/Ss on the optimal configuration of the network, if the S/Ss have the same configuration and their components are in identical condition. The upstream network can be seen in Fig. 6. The condition of all network components was assumed to be 0.5 p.u., which corresponds to average failure rates (taken from Fig. 2). Using these failure rates, the S/S failure rates were calculated using the methodology described in Section 3, and are shown in Table 6. These S/S failure rates do not include the failure rates of active faults on main feeder sections in combination with a stuck feeder CB, because they change depending on network configuration. However, they are considered when determining the optimal DS configuration.

The failure rates of S/Ss 2 and 3 are significantly higher than that of S/S 1. This is because S/Ss 2 and 3 are supplied by the high voltage busbar of S/S 1, therefore all failure events that cause the outage of this busbar also lead to the outage of S/Ss 2 and 3.

Optimal configurations were found using two objective functions: Total Cost 1 did not account for failures caused by components at S/Ss and the upstream network. Total Cost 2 considered the total ECOST and resulted in a different optimal configuration. This was due to a load

Table 7
Optimal configuration for the RBTS Bus 4 DS (Test Case 1).

Configuration	Original	min Total Cost 1	min Total Cost 2
Open branches	68–72	68–72	68–71, 41
$ECOST_1$ ($/yr)	102,114	102,114	104,085
$ECOST_2$ ($/yr)	77,196	77,196	72,392
ECOST ($/yr)	179,310	179,310	176,477
Loss (kW)	730.86	730.86	742.14
Loss Cost ($/yr)	131,555	131,555	133,585
Total Cost 1 ($/yr)	233,669	233,669	237,670
Total Cost 2 (f) ($/yr)	310,865	310,865	**310,062**

Table 8
Condition scores and failure rates of substation components (Test Case 2).

Substation component	S/S 1		S/S 2		S/S 3	
	Condition (p.u.)	Failure rate (f/yr)	Condition (p.u.)	Failure rate (f/yr)	Condition (p.u.)	Failure rate (f/yr)
Transformers	0.26	0.020	0.86	0.100	0.26	0.020
33 kV Busbar	0.35	0.005	0.67	0.020	0.35	0.005
11 kV Busbar	0.35	0.005	0.67	0.020	0.35	0.005
33 kV CBs	0.37	0.002	0.74	0.008	0.37	0.002
11 kV CBs	0.44	0.008	0.75	0.025	0.44	0.008

Table 9
Substation failure rates (Test Case 2).

Substation	S/S 1	S/S 2	S/S 3
Failure rate (f/yr)	0.1532	0.5319	0.2785

Table 10
Optimal configuration for the RBTS Bus 4 DS (Test Case 2).

Configuration	min Total Cost 1	min Total Cost 2
Open branches	68–72	68–71, 41
$ECOST_1$ ($/yr)	102,432	104,220
$ECOST_2$ (S/S 1) ($/yr)	13,059	17,762
$ECOST_2$ (S/S 2) ($/yr)	43,209	26,882
$ECOST_2$ (S/S 3) ($/yr)	18,032	18,032
$ECOST_2$ (Total) ($/yr)	74,300	62,676
ECOST ($/yr)	176,732	166,896
Loss (kW)	730.86	742.14
Loss Cost ($/yr)	131,555	133,585
Total Cost 1 ($/yr)	233,987	237,805
Total Cost 2 (*f*) ($/yr)	308,287	**300,481**

transfer from S/S 2, which had a higher failure rate and ECOST, to S/S 1, which had the lowest failure rate and ECOST. The results for this test case are shown in Table 7.

The optimal configuration of the network changed with the objective function. Specifically, LPs 24 and 25 (0.415 MW each, office buildings) were transferred from S/S 2 to S/S 1 by closing branch 72 and opening branch 41. This change increased the cost of losses (+2030 $/yr) and $ECOST_1$ (+1971 $/yr), but reduced the $ECOST_2$ (-4,804 $/yr). This led to an overall cost reduction of 803 $/yr, which rose to 1389 $/yr, if LPs 24 and 25 were increased to 1 MW.

5.1.2. Test Case 2

This test case examined the impact of of S/S component condition on optimal network configuration. The main assumption of this test case was that S/S 2 was in worse condition than the other S/Ss, as illustrated by the condition scores (and associated failure rates) shown in Table 8. The condition of all other components was considered to be 0.5 p.u.. According to the condition-based failure rates of all S/S components, the failure rate of each S/S was calculated; these are shown in Table 9. As in Test Case 1, the optimal configurations for minimum Total Cost 1 and Total Cost 2 were compared, and the results are presented in Table 10.

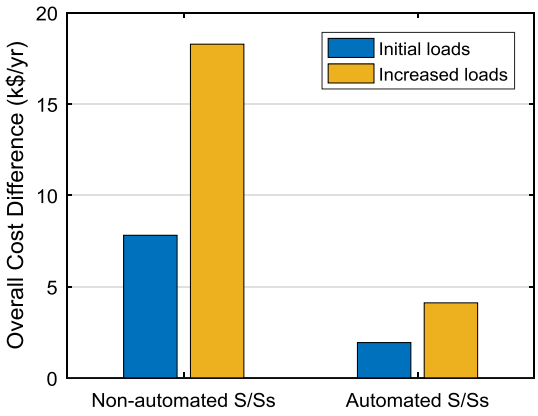

Fig. 9. Summary of Test Case 2 Results.

Table 10 shows that the minimization of Total Cost 2 resulted in a different optimal configuration, according to which LPs 24 and 25 (0.415 MW, office buildings), as well as 28 (1 MW, industrial) were transferred from S/S 2 to S/S 1. This load transfer reduced $ECOST_2$ (S/S 2) by 16,327 $/yr, and increased $ECOST_2$ (S/S 1) by only 4703 $/yr. The difference in the overall cost ($Cost_{Ploss}$ + ECOST) of the two aforementioned network configurations was 7806 $/yr. This difference rose to 18,267 $/yr, when LPs 24 and 25 were increased to 1 MW each. The process was repeated, with the S/Ss considered to be automated with a switching time of 10 min. The cost reductions became 1929 $/yr and 4106 $/yr for the initial and increased loads, respectively; these results are illustrated in Fig. 9.

5.2. Taiwan Power Company (TPC) DS

In the second case study, the proposed methodology was applied on a real-world DS operated by Taiwan Power Company (TPC) [13], shown in Fig. 10. This network is an 11.4 kV DS supplied by two S/Ss. It has 11 feeders, 83 normally closed branches and 13 normally open branches.

The following modifications and assumptions were made for the TPC DS:

(1) Customer types for all LPs were considered as shown in Table 11;
(2) Subtransmission lines were assumed to be 10 km long;
(3) The ratio between peak and average load was considered 1.63, as in [38];
(4) LPs 55 and 72 were increased to 1 MW;
(5) Alternative supply was available for all LPs (after switching) with the exception of LPs 8–10 and 21–24, for which there were a number of branch failures which led to an interruption until the failed component was repaired;
(6) Branch failure rates were calculated using the considered conductor type and branch resistances.

5.2.1. Test Case 3

This test case demonstrated the effect of S/S configuration on DSR. The assumed S/S configurations (see Fig. 5) were as follows: configuration (a) was used for S/S 1 and configuration (b) for S/S 2. The low voltage busbar of S/S 1 supplied feeders A-F and the split low voltage busbar of S/S 2 supplied feeders G-I on one side (S/S 2a) and feeders J and K on the other side (S/S 2b); these are illustrated in Fig. 11.

Taking the S/S configurations into account, and assuming a condition of 0.5 p.u. for all network components, S/S failure rates were computed (see Table 12). S/S 2 had a higher failure rate than S/S 1 because of the combination of the split low voltage busbar and the long

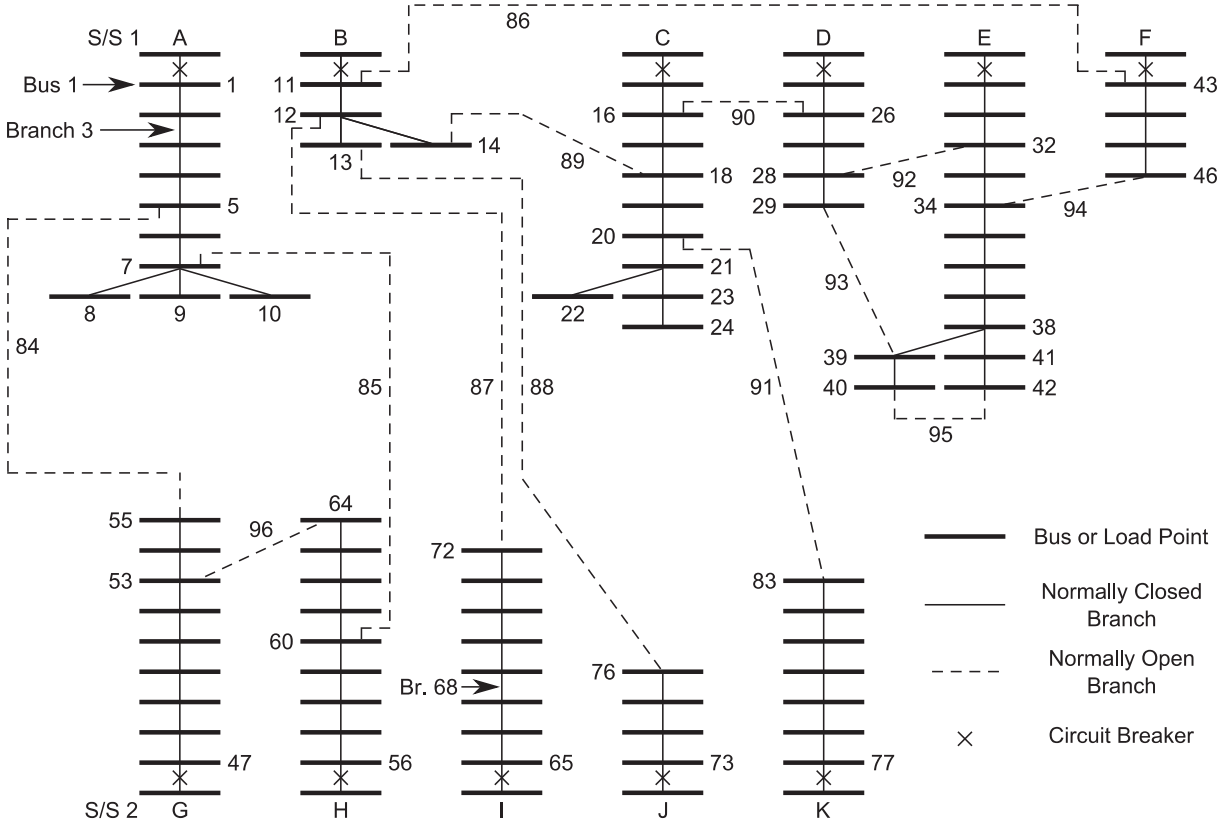

Fig. 10. TPC DS.

Table 11
Load types for the TPC DS.

Load type	Residential	Commercial	Industrial	Office buildings
Bus	2–4, 6, 8–10, 17–20, 22–28, 31, 34–42, 44, 45, 50, 51, 57, 59–62, 66, 71, 79, 80, 82	5, 7, 16, 21, 29, 32, 33, 46, 52–54, 63, 64, 68, 78, 83	12–14, 75, 76	55, 58, 72, 81

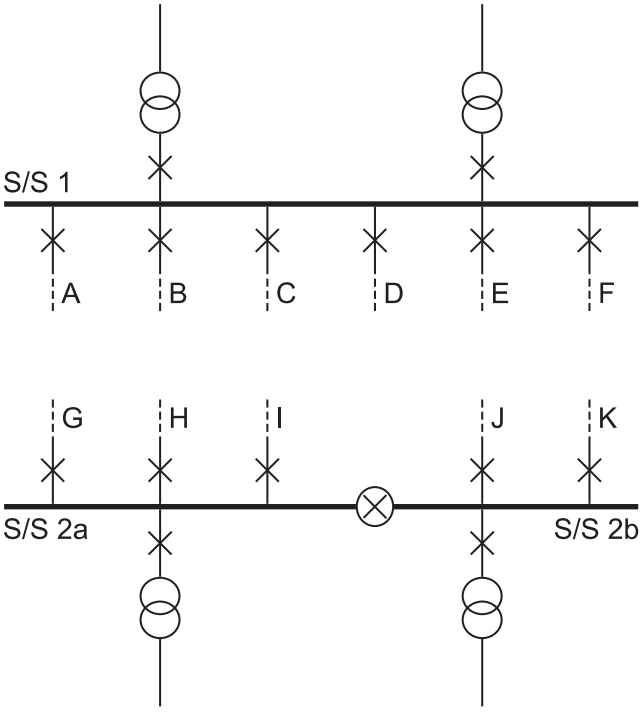

Fig. 11. Substation configurations for Test Case 3.

Table 12
Substation failure rates (Test Case 3).

Substation	S/S 1	S/S 2a	S/S 2b
Failure rate (f/yr)	0.1337	0.5270	0.5200

subtransmission lines (10 km). The optimal network configurations for Test Case 3 are shown in Table 13.

The higher failure rates of S/S 2 compared to S/S 1 led to a load transfer from the former to the latter; LPs 55 and 72 (1 MW each, office buildings) were transferred by closing branches 84 and 87, and opening branches 55 and 72. The $ECOST_2$ (S/S 2) reduction due to this load transfer was 23,913 $/yr, and the $ECOST_2$ (S/S 1) increase was 6,067 $/yr; considering S/S reliability within the DSR formulation led to a cost reduction of 11,025 $/yr.

5.2.2. Test Case 4

This test case considered the influence of primary DS component condition on optimal DSR by comparing the optimal configuration from min Total Cost 1, which ignored component condition, to its counterpart from min Total Cost 2, which took component condition into account. In this test case, branch 68 (here considered as underground cable) was considered to be in deteriorated condition, specifically 0.9 p.u. – corresponding to a failure rate of 1.0635 f/yr (assuming a cable resistance of 0.086 Ω/km). The condition of all other primary DS

Table 13
Optimal configuration for the TPC DS (Test Case 3).

Configuration for:	Original	min Total Cost 1	min Total Cost 2
Open branches	84–96	7, 34, 36, 42, 63, 83, 84, 86–90, 92	7, 34, 36, 42, 55, 63, 72, 83, 86, 88–90, 92
$ECOST_1$	78,731	76,130	85,147
$ECOST_2$ (S/S 1)	6,949	6,886	12,953
$ECOST_2$ (S/S 2a)	44,131	46,319	22,406
$ECOST_2$ (S/S 2b)	17,984	16,068	16,068
$ECOST_2$	69,064	69,273	51,427
ECOST	147,795	145,403	136,573
Loss (kW)	591.57	542.83	530.63
Loss Cost	106,483	97,709	95,513
Total Cost 1	185,214	173,839	180,660
Total Cost 2 (*f*)	254,278	243,112	**232,087**

Table 14
Optimal configuration for the TPC DS (Test Case 4).

Network configuration for:	min Total Cost 1	min Total Cost 2
Open branches	7, 34, 36, 42, 63, 83, 84, 86–90, 92	7, 34, 36, 42, 63, 72, 83, 84, 86, 88–90, 92
$ECOST_1$ ($/yr)	111,708	95,256
$ECOST_2$ ($/yr)	21,985	22,135
ECOST ($/yr)	133,693	117,391
Loss (kW)	542.83	528.52
Loss Cost ($/yr)	97,709	95,134
Total Cost 1 ($/yr)	209,417	190,390
Total Cost 2 (*f*) ($/yr)	231,402	**212,525**

components was considered to be 0.5 p.u.. It should be noted that if condition data are available for a number of components, then all of them can be used in order to inform the optimization algorithm. In this test case, only one branch was assumed to be in a condition other than average. This is because one is enough to indicate the impact of the condition of primary DS components on DSR. The optimization results for the present test case are shown in Table 14.

The high condition-based failure rate of branch 68 led to the transfer of LP 72 (1 MW, office buildings) from feeder I to feeder B. This transfer can be justified through the failure rate and the ECOST of LP 72 for the two configurations. In the first case, LP 72 was connected to feeder I, and its failure rate was 1.3031 f/yr; in the second case, it was connected to feeder B and the failure rate fell to 0.3783 f/yr, reducing the ECOST of this LP by 20,982 $/yr. Table 14 shows that the overall cost reduction through taking component condition into account, was 18,877 $/yr.

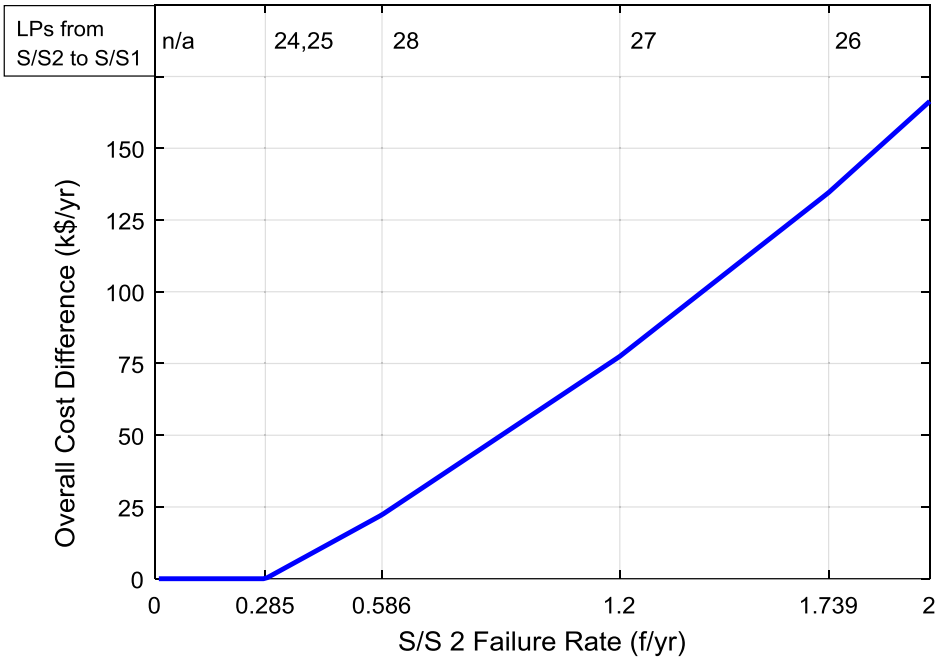

Fig. 12. Sensitivity analysis of S/S 2 failure rate on the overall cost difference and thresholds at which LPs are transferred from S/S2 to S/S1.

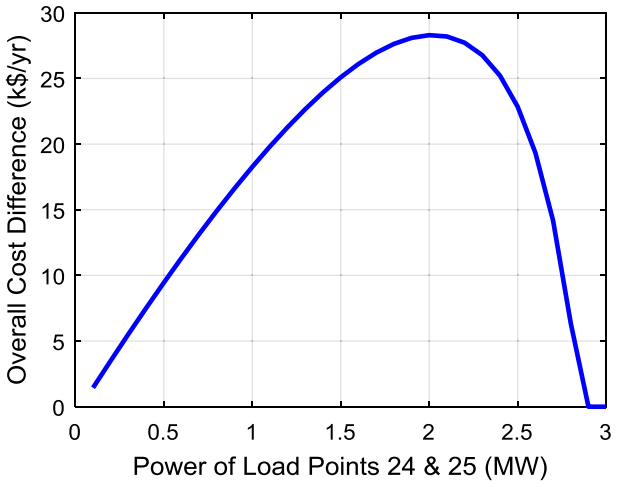

Fig. 13. Sensitivity analysis of power of load points 24 & 25 on the overall cost difference.

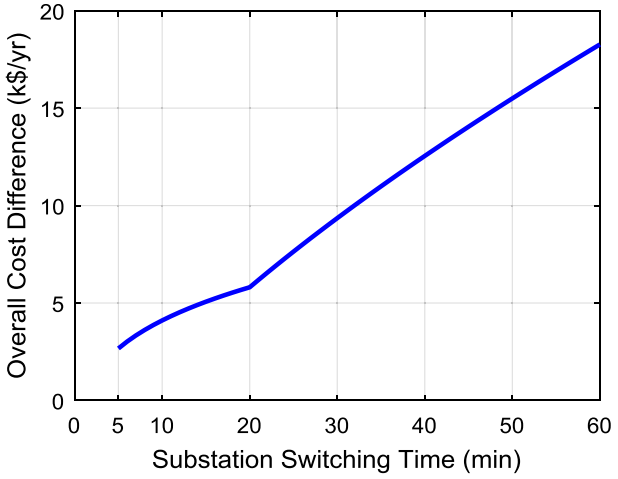

Fig. 14. Sensitivity analysis of substation switching time on the overall cost difference.

5.3. Sensitivity analysis

A sensitivity analysis was conducted to investigate how overall cost difference is influenced by three parameters:

(1) S/S 2 failure rate;
(2) power demand of LPs 24 and 25;
(3) S/S switching time (which is related to S/S automation).

The sensitivity analysis was carried out using Test Case 2, with increased loading for LPs 24 and 25. The corresponding results are illustrated in Figs. 12–14.

Increasing S/S 2 failure rate also increased the difference between the failure rates of S/Ss 1 and 2 (given that S/S 1 failure rate was kept constant), which caused the increase in the overall cost difference. Moreover, as the failure rate of S/S 2 increased, the optimal configuration of the network changed. Consequently, Fig. 12 is divided into five segments, which represent five different network configurations: when the failure rate reached given thresholds, LPs were transferred from S/S2 to S/S1, as illustrated in the figure.

As the demand of LPs 24 and 25 was increased up to 2 MW each, the overall cost difference became greater as well, as illustrated in Fig. 13. This was due to the difference in the S/S failure rates; more load was transferred, leading to higher reduction in ECOST. However, for demands greater than 2 MW, the overall cost difference started to decline, because the increase in loss cost was greater than the corresponding decrease in ECOST. It should also be mentioned that the load transfer is no longer worthwhile for demands greater than 2.9 MW; in this case the optimal configuration is the original one.

The variation of S/S switching time did not lead to a change in the optimal configuration of the network. However, the greater the S/S switching time, the greater the overall cost difference, as can be seen in Fig. 14; this shows that the proposed methodology can have a greater value in the case of no automated substations. The change in the slope at 20 min occurs because the ECOST calculation is different for outage durations between 1–20 min and 20–60 min.

Table 15
Comparison of integer GA and DPSO for test cases 2 and 3.

Test case number	Optimization method	Best Total Cost 2 (k$/yr)	Iteration (obtaining result)	Computational time (s)
2	Integer GA	300.48	6	64
	DPSO	300.48	13	76
3	Integer GA	232.09	42	166
	DPSO	232.95	34	152

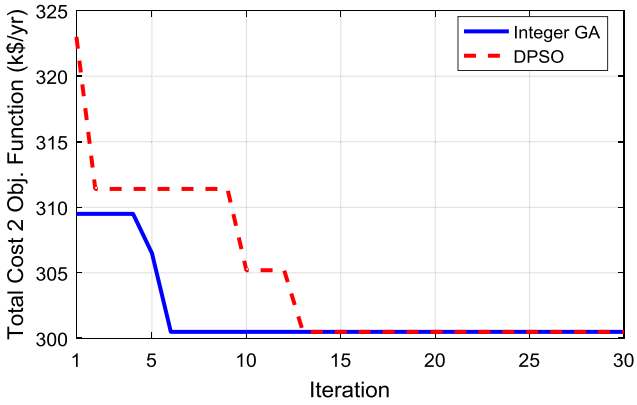

Fig. 15. Convergence graph of Total Cost 2 objective function using Integer GA and DPSO (Test Case 2).

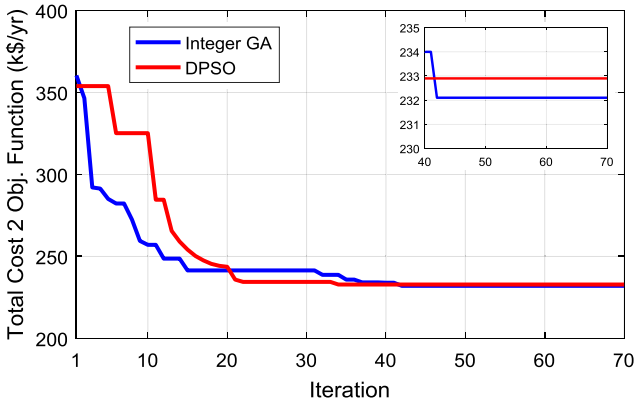

Fig. 16. Convergence graph of Total Cost 2 objective function using Integer GA and DPSO (Test Case 3).

5.4. Performance of integer GA and comparison with discrete PSO

This section describes the performance of the optimization algorithm used in this paper; and also provides a comparison with a discrete PSO (DPSO) [12] using the same values for the population size (swarm

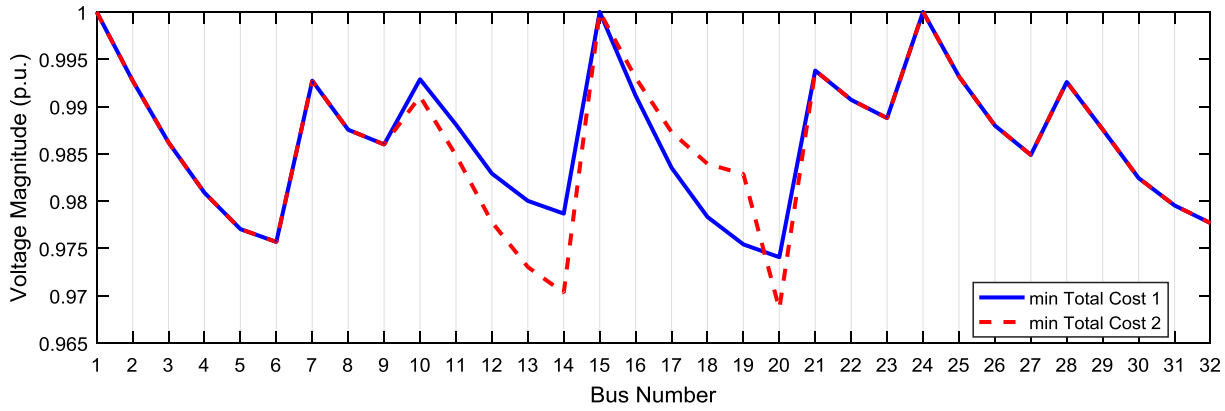

Fig. 17. Voltage profiles for Test Case 2.

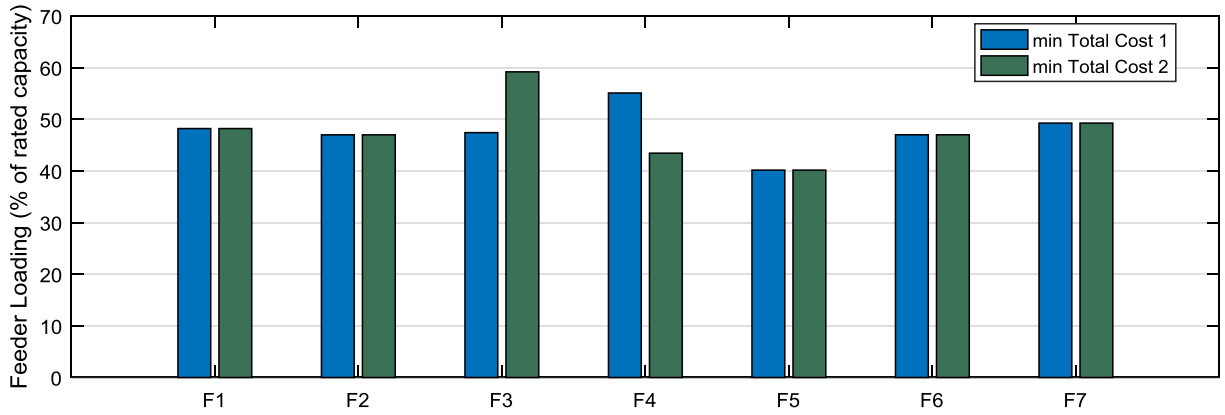

Fig. 18. Feeder loading for Test Case 2.

Table 16
System indices for bus voltages and feeder loading (Test Case 2).

Objective function	Min. voltage magnitude (p.u.)	Mean voltage magnitude (p.u.)	Mean feeder loading (% of capacity)	Load balance index [5]
Total Cost 1	0.9741	0.9863	47.72	1.6057
Total Cost 2	0.9686	0.9860	47.74	1.6164

size), maximum iterations, maximum stall iterations, and number of runs (see Table 5). The results are presented in Table 15 for Test Cases 2 and 3; the associated convergence graphs are illustrated in Figs. 15 and 16. The simulations were performed using an Intel Core i5 quad-core processor at 3.2 GHz and 8 GB of RAM.

In Test Case 2, the same optimal solution was obtained, and Integer GA required fewer generations to find the optimal configuration. In Test Case 3 (which used a practical DS), DPSO was quicker; however, it produced a worse solution than Integer GA. This can be justified by the fact that an improved GA and modified for integer and mixed integer optimization has been used in this paper (see Section 4.2).

5.5. Voltage profiles and feeder loading

This section analyzes the impact of network reconfiguration on voltage and feeder loading with and without considering component condition and S/S reliability; the analyses are carried out using Test Cases 2 and 3, and are presented in Sections 5.5.1 and 5.5.2, respectively. It should be noted that min Total Cost 2 corresponds to DSR, which considers component condition and S/S reliability, whereas the min Total Cost 1 objective function does not account for these factors.

5.5.1. Test Case 2 (RBTS Bus 4 DS)

The results for Test Case 2 are illustrated in Figs. 17 and 18, as well as Table 16. In this test case, LPs 24 and 25 were transferred from feeder F4 (of S/S 2, which had a high failure rate) to feeder F3 (of S/S 1, which was more reliable). This load transfer reduced the loading on feeder F4, and improved its voltage profile; however, it increased the loading on feeder F3, as well as its voltage profile deteriorated. After the load transfer, feeder F3 became longer (six main feeder sections – 19, 21, 23, 26, 28, and 72) and supplied two more LPs; therefore, network losses increased and this is why minimum voltage was lower and network loading was (slightly) higher. This happened because the feeders of this network were connected to each other only at their endpoints; more normally open branches could provide better reconfiguration options (as in Test Case 3). Nevertheless, if the minimum voltage reached an unacceptable value after the load transfer, the transformer tap changer at the S/S would be able to resolve this issue. Note that as far as the network loading is concerned, only the first branch of each feeder has been considered, i.e. branches 1, 13, 19, 31, 44, 50, and 56. This is because the first branch of each feeder experiences the heaviest loading between all feeder sections.

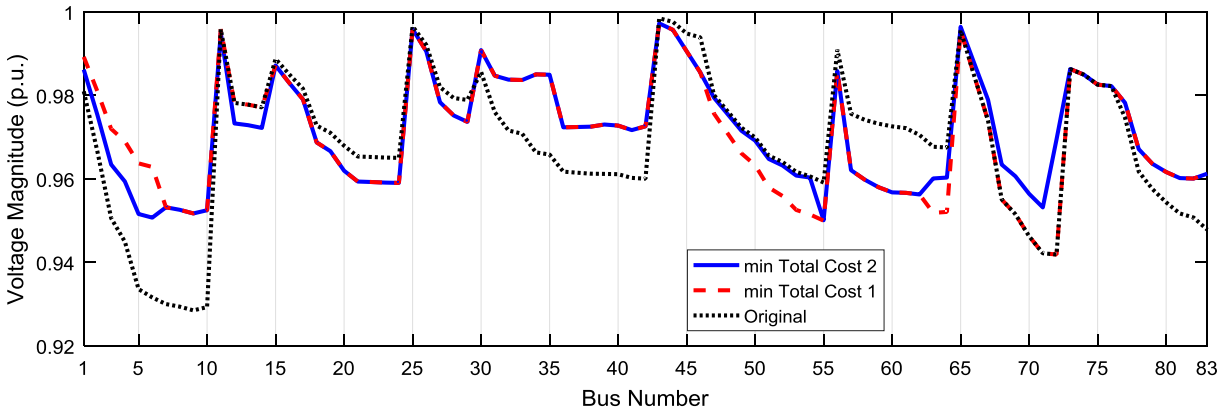

Fig. 19. Voltage profiles for Test Case 3.

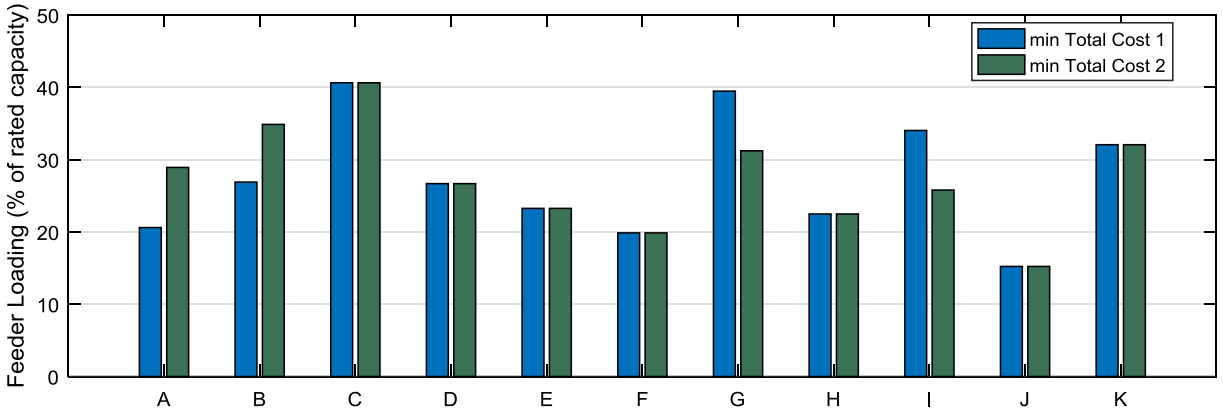

Fig. 20. Feeder loading for Test Case 3.

Table 17
System indices for bus voltages and feeder loading (Test Case 3).

Network configuration	Min. voltage magnitude (p.u.)	Mean voltage magnitude	Mean feeder loading (% of capacity)	Load balance index
Original	0.9285	0.9682	27.46	0.9295
min Total Cost 1	0.9419	0.9702	27.38	0.8926
min Total Cost 2	0.9501	0.9711	27.36	0.8754

5.5.2. Test Case 3 (TPC DS)

The network used in Test Case 3 (TPC DS) offered many more reconfiguration options than Test Case 2, because it had more normally open branches, which connected several points of a feeder to other feeders of both S/Ss. In this test case, LPs 55 and 72 were transferred from feeders G and I (of S/S 2a, which had a high failure rate) to feeders A and B (of S/S 1, which was more reliable), respectively. The results for this test case are illustrated in Figs. 19 and 20, as well as Table 17. LPs 55 and 72 were connected at the ends of the (relatively) highly loaded feeders G and I; this also caused high voltage drops along these feeders – bus 72 had the minimum voltage magnitude (0.942 p.u.) for min Total Cost 1 configuration. The transfer of these LPs substantially improved the voltage magnitude (0.97 p.u.) at bus 72, as well as balanced the loading between feeders G and A; network losses were also reduced.

Taking the above into consideration, the inclusion of component condition and S/S reliability into DNR may lead to better or worse voltage profile and load balance of the network; however, a greater number of reconfiguration options – in terms of feeder interconnections between each other – can help finding an optimal solution with improved bus voltages and feeder loadings.

6. Conclusion

This paper proposes a new, better informed, methodology for DSR, which minimizes the total cost of active power losses and ECOST by making use of component condition data and considering S/S reliability. Typically in network reconfiguration studies, average failure rates based on component type are used and S/S reliability is ignored. In this paper, condition-based failure rates are employed and the reliability of each S/S is taken into account. S/S reliability is determined by three factors: component condition, S/S configuration, and the upstream network. Moreover, each LP of the DS is assumed to have its own CDF, which depends on its type. The major conclusion of this paper is that there is significant value in incorporating component condition and S/S reliability into the DSR problem. Particularly, the inclusion of these factors in the optimization process leads to a better informed optimal network configuration. This is shown by the successful application of the proposed methodology to the RBTS Bus 4 DS and on a practical DS of Taiwan Power Company. The annual savings, compared to the formulation that neglects component condition and S/S reliability, can be in the order of tens of thousands of U.S. dollars for a single DS.

In general, the proposed methodology can be used in order to examine if there is value in changing the configuration of a DS. This can be done, for example, if new condition data become available to the DSO, or in the case of an outage – planned or unplanned – of an S/S transformer. It is expected that it will be more beneficial if there is a difference in the reliability of the S/Ss. If all S/Ss are considered identical, then the inclusion of the aforementioned factors will not change the optimal network configuration. However, if there are differences because of component condition, S/S configuration, and/or upstream network, then the optimal configuration of the network might be different, especially if there are LPs with high interruption costs that can potentially be transferred to other S/Ss.

It is also not necessary to have information for all condition parameters; the ones, for which there is information can be evaluated and a default score can be assigned to the rest of the parameters. However, as has already been mentioned, Ofgem has recently approved a common methodology [35] across all UK DSOs for the assessment of component condition and risk. This will encourage DSOs to collect and utilize condition data in a more organized way; therefore they will obtain a better knowledge of the condition of their assets, which could clearly facilitate the application of the proposed methodology to a DS.

Acknowledgments

This work was supported by the Engineering and Physical Sciences Research Council (EPSRC), UK (award reference 1645763) and Siemens plc, UK (reference 14220176). The authors would like to thank four anonymous reviewers for their valuable comments, as well as Dr Graeme Coapes from Siemens plc, Hebburn for his helpful feedback. Data supporting this publication is openly available under an 'Open Data Commons Open Database License'. Additional metadata are available at: http://dx.doi.org/10.17634/154300-106.

Appendix A

See Table A1.

Table A1
Reliability analysis for S/S configuration (a) – No automation/No alternative supply.

Failure event	λ (f/yr)	*r* (hr)	ECOST (k$/yr)
First-order total outages			
7	1.00×10^{-3}	2.00	0.1121
Second-order total outages			
1 + 4	9.66×10^{-5}	4.00	0.0199
1 + 5	9.06×10^{-6}	5.22	0.0026
1 + 6	1.89×10^{-6}	2.67	0.0002
2 + 4	9.06×10^{-6}	5.22	0.0026
2 + 5	7.71×10^{-7}	7.50	0.0003
2 + 6	1.95×10^{-7}	3.16	0.0000
3 + 4	1.89×10^{-6}	2.67	0.0002
3 + 5	1.95×10^{-7}	3.16	0.0000
3 + 6	3.29×10^{-8}	2.00	0.0000
Subtotal	1.20×10^{-4}	4.16	0.0261
Second-order total outages (m)	1.12×10^{-2}	7.56	5.2791
Active failures			
3A	4.00×10^{-3}	1.00	0.2520
6A	4.00×10^{-3}	1.00	0.2520
F4 CB	4.00×10^{-3}	1.00	0.2520
F5 CB	4.00×10^{-3}	1.00	0.2520
Subtotal	1.60×10^{-2}	1.00	1.0081
Active failures and stuck CB			
1A + 3S	1.15×10^{-2}	1.00	0.7246
2A + 3S	7.50×10^{-4}	1.00	0.0473
4A + 6S	1.15×10^{-2}	1.00	0.7246
5A + 6S	7.50×10^{-4}	1.00	0.0473
(31, 33, 36, 39, 41)A + F4 CB S	1.24×10^{-2}	1.00	0.7781
(44, 46, 48)A + F5 CB S	7.00×10^{-3}	1.00	0.4410
Subtotal	4.39×10^{-2}	1.00	2.7628
Total	7.22×10^{-2}	2.04	9.1878

References

[1] Billinton R, Allan RN. Reliability evaluation of power systems. 2nd ed. New York: Plenum; 1996.
[2] Brown RE. Electric power distribution reliability. New York: Marcel Dekker; 2002.
[3] Brown RE, Burke JJ. Managing the risk of performance based rates. IEEE Trans Power Syst May 2000;15:893–8.
[4] Zhu J. Optimization of power system operation. 2nd ed. New Jersey: Wiley-IEEE Press; 2015.
[5] Baran ME, Wu FF. Network reconfiguration in distribution systems for loss reduction and load balancing. IEEE Trans Power Del 1989;4(Apr.):1401–7.
[6] Ch Y, Goswami SK, Chatterjee D. Effect of network reconfiguration on power quality of distribution system. Int J Elect Power Energy Syst 2016;83(Dec.):87–95.
[7] Ghofrani-Jahromi Z, Kazemi M, Ehsan M. Distribution switches upgrade for loss reduction and reliability improvement. IEEE Trans Power Del 2015;30(Apr.):684–92.
[8] Tahboub AM, Pandi VR, Zeineldin HH. Distribution system reconfiguration for annual energy loss reduction considering variable distributed generation profiles. IEEE Trans Power Del 2015;30(Aug.):1677–85.
[9] Asrari A, Lotfifard S, Ansari M. Reconfiguration of smart distribution systems with time varying loads using parallel computing. IEEE Trans Smart Grid 2016;7(Nov.):2713–23.
[10] Amanulla B, Chakrabarti S, Singh SN. Reconfiguration of power distribution systems considering reliability and power loss. IEEE Trans Power Del 2012;27(Apr.):918–26.
[11] Guan W, Tan Y, Zhang H, Song J. Distribution system feeder reconfiguration considering different model of DG sources. Int J Elect Power Energy Syst 2015;68(Jun.):210–21.
[12] Li Z, Jazebi S, de León F. Determination of the optimal switching frequency for

distribution system reconfiguration. IEEE Trans Power Del 2017;32(Aug.):2060–9.
[13] Su C-T, Chang C-F, Chiou J-P. Distribution network reconfiguration for loss reduction by ant colony search algorithm. Elect Power Syst Res 2005;75(Aug.):190–9.
[14] Nguyen TT, Truong AV. Distribution network reconfiguration for power loss minimization and voltage profile improvement using cuckoo search algorithm. Int J Elect Power Energy Syst 2015;68(Jun.):233–42.
[15] Nguyen TT, Truong AV, Phung TA. A novel method based on adaptive cuckoo search for optimal network reconfiguration and distributed generation allocation in distribution network. Int J Elect Power Energy Syst 2016;78(Jun.):801–15.
[16] Sudha Rani D, Subrahmanyam N, Sydulu M. Multi-objective invasive weed optimization – an application to optimal network reconfiguration in radial distribution systems. Int J Elect Power Energy Syst 2015;73(Dec.):932–42.
[17] Lotfipour A, Afrakhte H. A discrete Teaching–Learning-Based Optimization algorithm to solve distribution system reconfiguration in presence of distributed generation. Int J Elect Power Energy Syst 2016;82(Nov.):264–73.
[18] Schmidt HP, Ida N, Kagan N, Guaraldo JC. Fast reconfiguration of distribution systems considering loss minimization. IEEE Trans Power Syst 2005;20(Aug.):1311–9.
[19] Deep K, Singh KP, Kansal ML, Mohan C. A real coded genetic algorithm for solving integer and mixed integer optimization problems. Appl Math Comput 2009;212:505–18.
[20] Tang L, Yang F, Feng X. A novel method for distribution system feeder reconfiguration using black-box optimization. Proc IEEE power energy Soc Gen meeting Vancouver, BC, Canada. 2013.
[21] Brown RE. Distribution reliability assessment and reconfiguration optimization. Proc transmission and distribution Conf Expo. 2001.
[22] Paterakis NG, Mazza A, Santos SF, Erdinç O, Chicco G, Bakirtzis AG, et al. Multi-objective reconfiguration of radial distribution systems using reliability indices. IEEE Trans Power Syst 2016;31(Mar.):1048–62.
[23] Yin SA, Lu CN. Distribution feeder scheduling considering variable load profile and outage costs. IEEE Trans Power Syst 2009;24(May):652–60.
[24] Zhang P, Li W, Wang S. Reliability-oriented distribution network reconfiguration considering uncertainties of data by interval analysis. Int J Elect Power Energy Syst 2012;34(Jan.):138–44.
[25] Kavousi-Fard A, Niknam T. Optimal distribution feeder reconfiguration for reliability improvement considering uncertainty. IEEE Trans Power Del 2014;29(Jun.):1344–53.
[26] Goel L, Billinton R. Evaluation of interrupted energy assessment rates in distribution systems. IEEE Trans Power Del 1991;6(Oct.):1876–82.
[27] Sarantakos I, Lyons P, Blake S, Taylor P, Tao L, Celik S, et al. Incorporating asset management into power system operations. CIRED – Open Access Proc J 2017;2017:1227–31.
[28] Hjartarson T, Otal S. Predicting future asset condition based on current health index and maintenance level. ESMO 2006 – 2006 IEEE 11th international conference on transmission & distribution construction, operation and live-line maintenance. 2006.
[29] Naderian A, Cress S, Piercy R, Wang F, Service J. An approach to determine the health index of power transformers. 2008 IEEE international symposium on electrical insulation. 2008.
[30] Jahromi A, Piercy R, Cress S, Service J, Fan W. An approach to power transformer asset management using health index. IEEE Electr Insul Mag, 2009;25:20–34.
[31] Siemens RCAM dynamic. Available: < https://www.energy.siemens.com/br/en/services/power-transmission-distribution-smart-grid/condition-monitoring/reliability-centered-asset-management.htm > .
[32] EA Technology CBRM. Available: < https://www.eatechnology.com/wp-content/uploads/2017/03/CBRM-brochure.pdf > .
[33] Brown RE, Frimpong G, Willis HL. Failure rate modeling using equipment inspection data. IEEE Trans Power Syst 2004;19(May):782–7.
[34] Hughes D, Pears T, Tian Y. Linking engineering knowledge and practical experience to investment planning by means of condition based risk management. 2008 International conference on condition monitoring and diagnosis. 2008.
[35] UK DNOs working group. DNO common network asset indices methodology; 2017.
[36] Billinton R, Allan RN. Reliability evaluation of engineering systems. 2nd ed. New York: Plenum; 1992.
[37] Billinton R, Kumar S, Chowdhury N, Chu K, Debnath K, Goel L, et al. A reliability test system for educational purposes-Basic data. IEEE Trans Power Syst 1989;4(Aug.):1238–44.
[38] Allan RN, Billinton R, Sjarief I, Goel L, So KS. A reliability test system for educational purposes – basic distribution system data and results. IEEE Trans Power Syst 1991;6(May):813–20.
[39] MathWorks. Mixed integer optimization; 2018. Available: < https://uk.mathworks.com/help/gads/mixed-integer-optimization.html > .
[40] Zimmerman RD, Murillo-Sánchez CE, Thomas RJ. MATPOWER: steady-state operations, planning, and analysis tools for power systems research and education. IEEE Trans Power Syst 2011;26:12–9.
[41] Shirmohammadi D, Hong HW, Semlyen A, Luo GX. A compensation-based power flow method for weakly meshed distribution and transmission networks. IEEE Trans Power Syst 1988;3(May):753–62.
[42] Zimmerman RD, Murillo-Sánchez CE. MATPOWER user's manual, Version 7.01b1; 2018. Available: < http://www.pserc.cornell.edu/matpower/manual.pdf > .